Journal of Atmospheric and Solar-Terrestrial Physics 94 (2013) 41–48

Contents lists available at SciVerse ScienceDirect

Journal of Atmospheric and Solar-Terrestrial Physics

journal homepage: www.elsevier.com/locate/jastp

Spatial and time distribution of the flash rate over tropical Africa

Rodrigo E. Bürgesser [a,*], Maria G. Nicora [b], Eldo E. Ávila [a]

[a] FaMAF, Universidad Nacional de Córdoba, IFEG-CONICET, Medina Allende s/n, Ciudad Universitaria, CP. X5000HUA, Córdoba, Argentina
[b] Centro de Investigaciones en Láseres y Aplicaciones (CITEFA-CONICET), San Juan Bautista de La Salle 4397, CP. B1603ALO, Villa Martelli, Argentina

ARTICLE INFO

Article history:
Received 15 October 2012
Received in revised form
5 December 2012
Accepted 31 December 2012
Available online 17 January 2013

Keywords:
Tropical Africa lightning
World Wide Lightning Location Network
Lightning imaging sensor

ABSTRACT

The lightning flash rate over tropical Africa was analyzed using lightning data of two independent lightning detection systems, the World Wide Lightning Location Network and the Lightning Imaging Sensor. Spatial and time distributions of lightning activity were studied using different spatial and temporal scales. Results show a very localized high-lightning activity center on the west side of the Albertine Rift Mountain, located east of the Congo Basin, and substantial lightning activity in the center of the region. Both centers show low variations on the lightning activity throughout the year and a marked diurnal cycle with a maximum lightning activity in the local afternoon. A secondary lightning activity center was found over Lake Victoria, which has an annual variation similar to that of the Congo Basin lightning activity centers but does not show a marked diurnal cycle. The lightning activities observed seem to be strongly influenced by topography and are in agreement with the small temperature ranges and with the rainfall observed in the region.

1. Introduction

Three zones have been long recognized as major components of the global electrical circuit (Whipple, 1929): Africa, South America and the Maritime Continent. These three zones stand out in all global maps of lightning activity with Africa dominating over the other two (Brooks, 1925; Christian et al., 1999; Boccippio et al., 2000; Christian et al., 2003).

There is a great deal of work related to the lightning activity over Africa with a clear agreement that it is mainly concentrated in the tropics with less intensity over South Africa and over the Mediterranean Sea coast in the north. In the tropical region, the Congo Basin shows the highest lightning activity followed by the Gulf of Guinea in the west and by the Ethiopian Highlands in the north-east. Albrecht et al. (2011) found a maximum flash rate of 232 fl km^{-2} yr^{-1} over the Congo Basin, which is the second high lightning activity center of the world after Lake Maracaibo (Bürgesser et al., 2012).

Several studies have analyzed the lightning activity over Africa and the Congo Basin by using satellite data. For instance, Williams and Satori (2004) used lightning data from the Optical Transient Detector (OTD) and from the Lightning Imaging Sensor (LIS), and found a pronounced semi-annual behavior in the flash rate for the Congo Basin, with maxima at equinox months (March, September) and a minimum in July. They reported an enhancement over the higher terrain on the eastern edge portion of the Congo basin. Nevertheless, the authors concluded that this was a small factor in the overall lightning activity. Collier and Hughes (2011a) derived annual lightning flash rate patterns for most African countries using superimposed annual and semi-annual sinusoidal components. For the Democratic Republic of Congo, these authors found intense lightning activity from November until March with an annual average lightning activity of 47.8 km^{-2} yr^{-1}. The amplitude of the annual variation was significantly smaller than the annual mean, indicating that there is an significant level of lightning activity throughout the year.

The lightning activity over tropical Africa, particularly over the Congo Basin, presents spatial and time distributions with some features which are not fully detected with satellite data. In this work, the World Wide Lightning Location Network (WWLLN) Stroke B data (Rodger et al., 2009) are used to examine the lightning activity over tropical Africa. By covering the region with a $0.1^\circ \times 0.1^\circ$ grid cell, the high lightning activity centers in the region were recognized and analyzed in terms of diurnal to inter-annual time scales.

2. Dataset

The lightning data used in this study came from two independent lightning detection systems, the World Wide Lightning Location Network (WWLLN) and the Lightning Imaging Sensor (LIS).

The WWLLN (http://wwlln.net) is a real-time, world-wide, ground network that detects preferentially strong lightning strokes.

* Corresponding author. Tel.: +54 351 4334051x416.
E-mail address: burgesse@famaf.unc.edu.ar (R.E. Bürgesser).

1364-6826/$ - see front matter © 2013 Elsevier Ltd. All rights reserved.
http://dx.doi.org/10.1016/j.jastp.2012.12.025

The WWLLN receivers detect the very low frequency (VLF) radiation (3–30 kHz) from a lightning stroke and use the time of group arrival (TOGA) to locate the position of the lightning. The propagation and low attenuation of VLF waves in the Earth-Ionosphere waveguide allows, with fewer antennas compared with other ground detection systems, a global and real-time detection of lightning activity (Dowden et al., 2002, 2008; Lay et al., 2004; Rodger et al., 2005; Jacobson et al., 2006).

The WWLLN had 20 stations at the beginning of 2004 and reached more than 55 stations during 2012. The stations consist of a 1.5 m whip antenna, a Global Positioning System (GPS) receiver, a VLF receiver, and a processing computer with Internet connection. Residual minimization methods are used in the TOGA data at the processing stations to create high quality data from lightning locations. The WWLLN data processing ensures that the residual time is less than 30 μs and that the data delivered by the network correspond to lightning strokes detected by at least five stations (Rodger et al., 2009). The lightning location accuracy of the network is ~5 km (Abreu et al., 2010).

The Lightning Imaging Sensor is a space-based instrument, on board the Tropical Rainfall Measurement Mission (TRMM) satellite (http://thunder.msfc.nasa.gov), specifically designed to continuously detect the total lightning activity, both intra-cloud (IC) and cloud to ground (CG) (Christian et al., 1999), of any given storm that passes through the field of view (600×600 km^2) of its sensor. The observation time of a given storm is 80 s. Since the TRMM satellite orbit has an inclination of 35°, the LIS instrument can only detect lightning activity between 35° north latitude and 35° south latitude. The LIS data used in this study belong to the period between 1998 and 2011 and include the spatial location of each flash (latitude, longitude) detected. Also, the data contain a grid, with spatial resolution of $0.5^\circ \times 0.5^\circ$, with the effective observation time of each grid cell. The total observation time for each cell is about 400,000 s.

The Cloud Top Temperature (CTT) and Air Surface Temperature (AST) data used come from the Atmospheric Infrared Sounder (AIRS). AIRS is an instrument on board the Aqua satellite, which is part of the NASA Earth Observing System (http://airs.jpl.nasa.gov/). AIRS measures the infrared brightness of the Earth's surface and atmosphere in 2378 spectral channels ranging from 3.7 to 15.4 mm (Chahine et al., 2006). The geophysical parameters have been averaged and binned into $1^\circ \times 1^\circ$ grid cells covering the entire globe. AIRS observations are neither simultaneous nor synchronous with LIS observations. The data used are version 5, level 3 products and correspond to the period between 2003 and 2008.

3. Results and discussions

Fig. 1 (Upper-Left Panel) shows the flash rate derived from LIS overpasses between January 1998 and December 2011 over Africa. A spatial resolution of $0.5^\circ \times 0.5^\circ$ was used on the map. This figure shows that the main lightning activity is confined in the tropical zone between 10°N and 10°S. The Congo Basin is located within this area and extends over six countries: Cameroon, Central African Republic, Congo, Democratic Republic of Congo, Equatorial Guinea and Gabon; it is well recognized that it has one of the highest rates of lightning activity in the world. The region presents a background lightning activity of 40 fl km^{-2} yr^{-1} and also shows a spatial distribution with centers of higher lightning activity on the eastern edge of the Congo Basin region and the central region with lightning activities larger than 80 fl km^{-2} yr^{-1}. The tropical lightning activity in Africa is enclosed by the Sahel and Sahara Deserts in the north and by high terrain elevations (>1000 m) in the south (Bie and Katanga Plateau) and east (Albertine Rift Mountain) as can be observed in Fig. 1 (Upper-Rigth Panel). The ground elevation data used in Fig. 1 (Upper-Right panel) were obtained from the Global Land One-kilometer Base

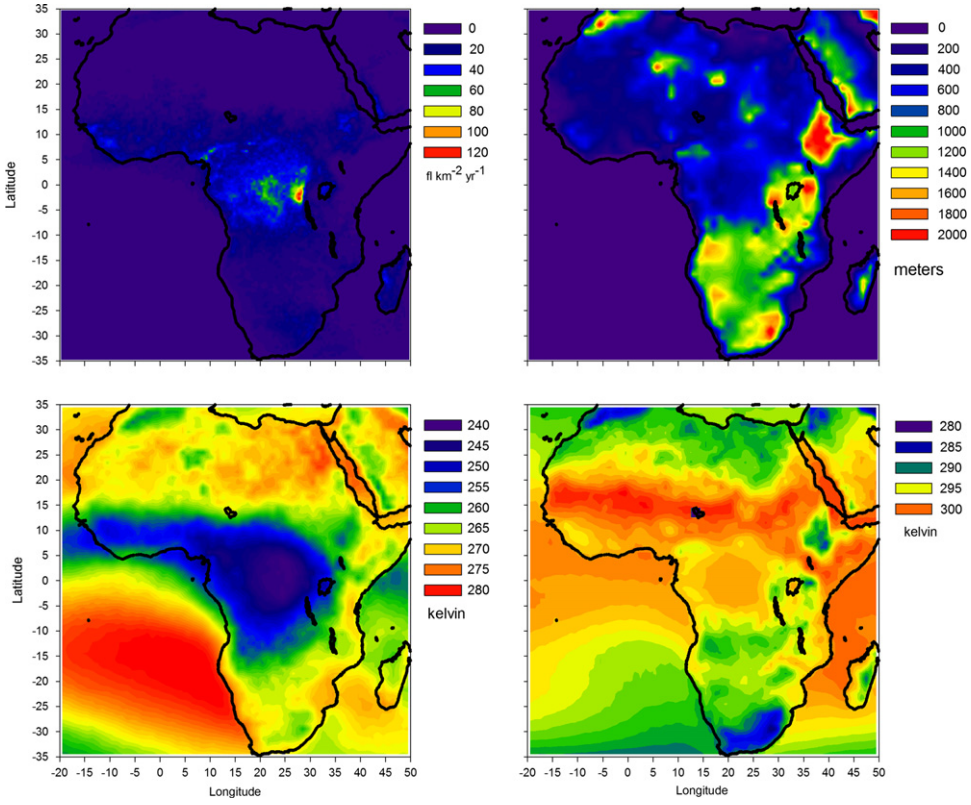

Fig. 1. Upper-Left Panel. Spatial distribution of the flash rate computed using LIS data between 1998 and 2011. Upper-Right Panel. Topography of the region with the color scale in meters over sea level (GLOBE). Lower-Left Panel. Main Cloud Top Temperature. Lower-Right Panel. Main Surface Temperature.

Elevation (GLOBE, http://www.ngdc.noaa.gov/mgg/topo/globe.html).

Fig. 1 also displays the annual mean CTT (Lower-Left Panel) and the annual mean AST (Lower-Right Panel) over Africa as measured by AIRS. The Congo Basin presents the lowest mean annual CTT over Africa with values colder than 250 K and a mean annual AST warmer than 300 K. The CTT is a good indicator of the vertical development of the cloud and low CTT values are usually related to deep convection (Fu et al., 1990; Liu et al., 1995; Hong et al., 2005; Aumann et al., 2007). Many studies indicate a strong link between lightning production and the microphysical and dynamical characteristics of the clouds, particularly deep convective clouds (DCC). The lightning activity in DCC is expected to depend on the intensity of vertical air motion, which is closely related to the storm height (Williams, 1985; Price and Rind, 1992; Ushio et al., 2001; Ávila et al., 2010). The Congo Basin seems to gather the most favorable thermodynamic conditions to produce deep convection; these are moisture, higher AST and lower CTT; which can lead to significant lightning activity.

Fig. 2 shows the flash rate detected by LIS (*FRLis*, Upper Panel) between 1998 and 2011 and by WWLLN during 2011 (*FRw*, Lower Panel) for the spatial windows between $[-10^\circ; 15^\circ]$ of latitude and $[10^\circ; 40^\circ]$ of longitude with a spatial resolution of $0.5^\circ \times 0.5^\circ$. Both maps also show the ground elevation contours with the same spatial resolution used in the lightning maps. As can be observed, both lightning maps show a similar spatial flash rate distribution with the center of high lightning activity in the east of the Congo Basin and the region with substantial lightning activity in the center of the region. The WWLLN detected a maximum flash rate of 4 fl km^{-2} yr^{-1} at the center of the high lightning activity area and 1.5 fl km^{-2} yr^{-1} on the central region, while LIS detected 135 fl km^{-2} yr^{-1} and 60 fl km^{-2} yr^{-1}, respectively. Assuming a detection efficiency for LIS of 0.85 (Boccippio et al., 2002), a detection efficiency of WWLLN over the Congo Basin region of 2–3% can be estimated. Clearly, this fairly low detection efficiency is a consequence of the low number of WWLLN stations in Africa, which means that only very high-peak current CGs were detectable in these regions. However, in spite of the low detection efficiency of WWLLN, both lightning datasets (WWLLN and LIS) show a good spatial correlation with a Pearson coefficient of 0.69 ($p < 10^{-4}$) and the WWLLN seems to be capable of detecting the main features of the lightning spatial distribution over the Congo Basin.

Fig. 2 displays once again that the region of lightning activity is limited by the high terrains (> 1000 m) on the south and east of the Congo Basin. The western and eastern border can be observed in Fig. 3 (Upper panel), where the profile of topography (blue dotted line) and the flash rate (black line) detected by LIS (*FRLis*) for a grid cell of $(0.5^\circ \times 0.5^\circ)$ centered at -1.75° of latitude and between $[5^\circ; 40^\circ]$ of longitude are presented. The profile shows low lightning activity at the western longitude ($< 10^\circ$) which corresponds to the Atlantic Ocean (zero meters ground elevation). Between $[10^\circ; 25^\circ]$ of longitude (Congo Basin) the African Continent presents a ground elevation of 500 m with substantial lightning activity (40–60 fl km^{-2} yr^{-1}). Toward the east, an increase

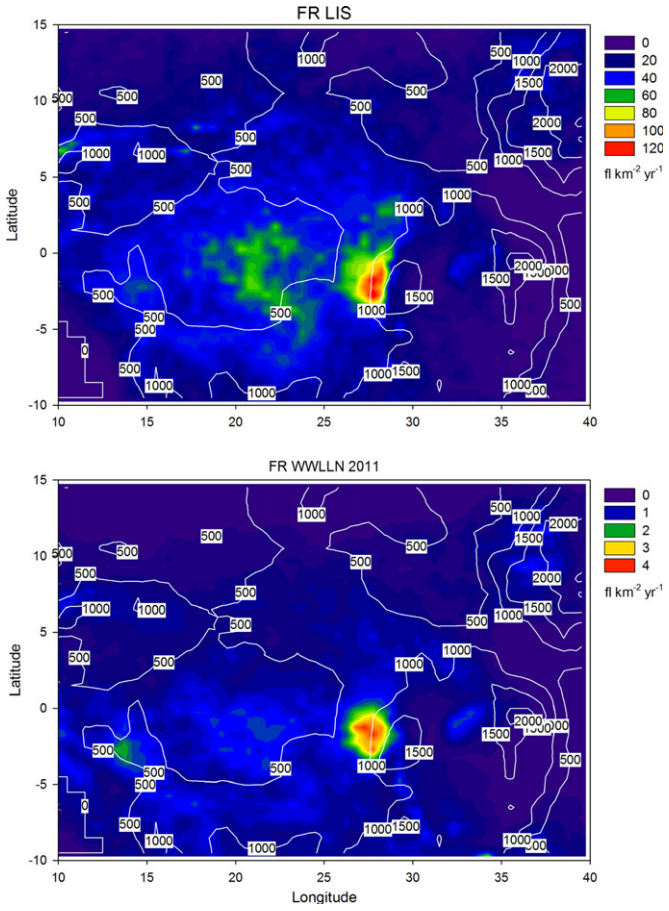

Fig. 2. Spatial distribution of the flash rate computed using LIS data (FRLis, Upper Panel) and WWLLN data (FRw, Lower Panel) and the height contours (GLOBE).

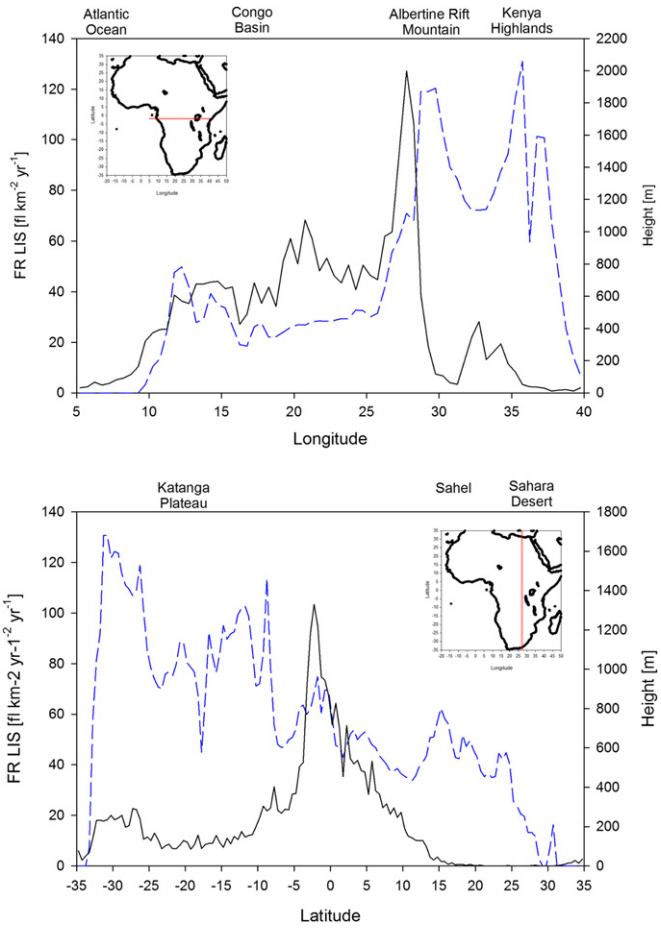

Fig. 3. Profile of topography (blue dashed line) and flash rate detected by LIS (solid line) for the grid cell of $(0.5^\circ \times 0.5^\circ)$ centered at -1.75° of latitude and between $[5^\circ; 40^\circ]$ of longitude (Upper Panel), for the grid cell of $(0.5^\circ \times 0.5^\circ)$ centered at 27.25° of longitude and between $[-35^\circ; 35^\circ]$ of latitude (Lower Panel). (For interpretation of the references to color in this figure caption, the reader is referred to the web version of this article.)

of the lightning activity is observed which is coincident with an increase in ground elevation. The flash rate shows a peak between [25°; 30°] of longitude, which corresponds to the center of lightning activity observed in Figs. 1 and 2. The peak is located at the west side of the Albertine Rift Mountain. Another peak with 20 fl km^{-2} yr^{-1} can also be observed between the Albertine Rift Mountain and the Kenya Highlands, between [31°; 35°] of longitude, which corresponds to the location of Victoria Lake.

Fig. 3 (Lower panel) shows the same as Fig. 3 (Upper panel) but for the grid cell of ($0.5° \times 0.5°$) centered at 27.25° of longitude and between [−35°; 35°] of latitude. For latitudes between −35° and −10°, the topography shows terrains with altitudes above 1000 m which correspond to the Katanga Plateau. These latitudes show lightning activity of less than 20 fl km^{-2} yr^{-1}. For latitudes between −5° and 5°, the lightning activity presents a peak with more than 100 fl km^{-2} yr^{-1} which corresponds to the high lightning activity center observed previously. Towards the north, the lightning activity decreases and reaches values of zero for latitudes greater than 15°, which correspond to the Sahel and Sahara Deserts.

In order to analyze the annual evolution of the spatial distribution of the lightning activity in the Congo Basin, the total flashes per year ($F_w[i,j]$) detected by the WWLLN in each grid point centered in [i,j] of latitude and longitude, with a spatial resolution of [$0.1° \times 0.1°$], were computed for each year between 2005 and 2011. In order to take into account the detection efficiency variation of WWLLN due to the addition of new antennas and upgrades on the detection algorithm, the values of $F_w[i,j]$ were normalized to the total flashes in the spatial window considered for the whole year ($\sum_i \sum_j F_w[i,j]$). Thus the parameter.

$$F_{w,n}(\text{year})[i,j] = \frac{F_w[i,j]}{\sum_i \sum_j F_w[i,j]}$$

is used as an indicator of the lightning activity on each grid point. Fig. 4 shows the spatial distribution of $F_{w,n}$ in the spatial windows between [−5°; 5°] of latitude and [20°; 30°] of longitude. For these spatial windows, the Pearson coefficient between the flash rate detected by LIS and by WWLLN during 2011 is 0.78 ($p < 10^{-4}$). In all the years analyzed, both the high-lightning

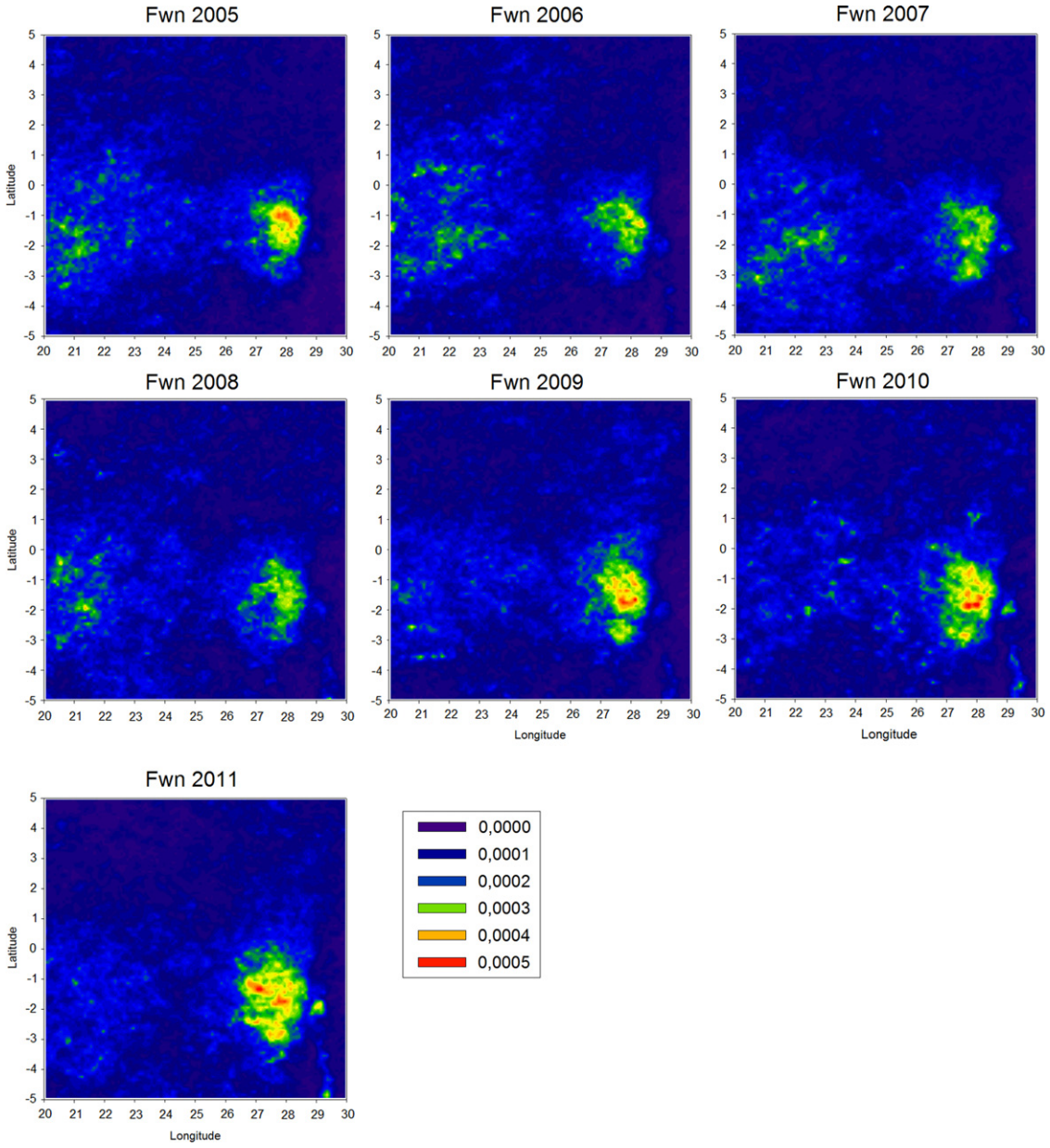

Fig. 4. Spatial distribution of $F_{w,n}$ values for the years between 2005 and 2011 for the Congo Basin.

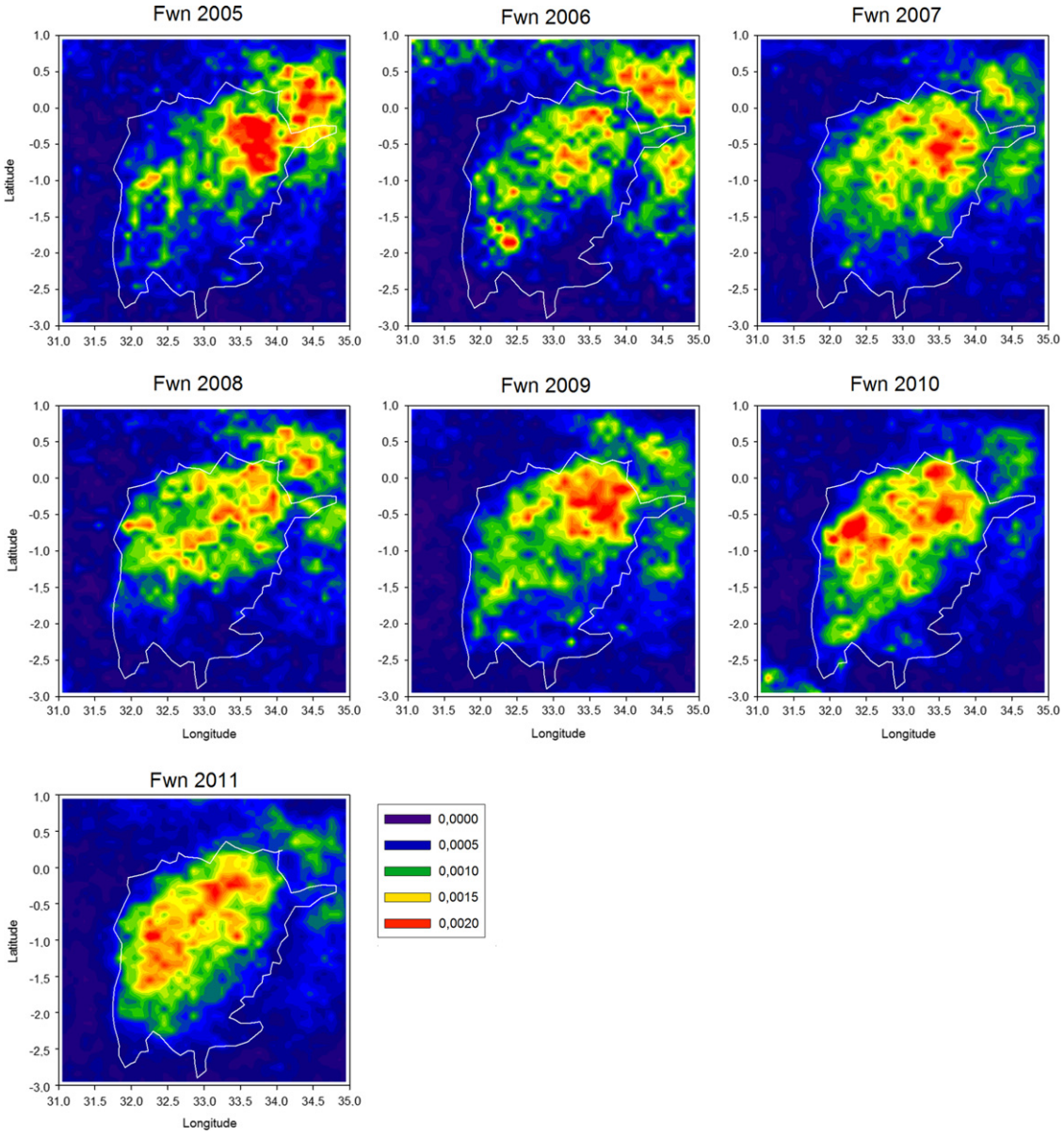

Fig. 5. Spatial distribution of $F_{w,n}$ values for the years between 2005 and 2011 for Lake Victoria.

activity region and the central region can be observed. The high-lightning activity center is confined between $[-3^{\circ}; 0^{\circ}]$ of latitude and $[26^{\circ}; 29^{\circ}]$ of longitude, while the central region presents a more disperse flash rate distribution and does not show a particular spatial distribution pattern.

Similarly to Fig. 4, Fig. 5 shows the annual lightning activity for the spatial windows between $[-3^{\circ}; 1^{\circ}]$ of latitude and $[31^{\circ}; 35^{\circ}]$ of longitude; the border observed in the figure corresponds to Lake Victoria. For every year analyzed, the results show that the lightning activity is largely confined over the lake, and over the northeast area, with less lightning activity over the south region of the lake. For this region, the lightning dataset from LIS and WWLLN give a good spatial correlation with a Pearson coefficient of 0.88 ($p < 10^{-4}$). The flash rate detected by LIS over Lake Victoria is higher than 30 fl km^{-2} yr^{-1} on the north area and around 10 fl km^{-2} yr^{-1} on the south area.

Using satellite data from LIS and OTD, Collier and Hughes (2011a) studied the climatologies of the lightning activity for

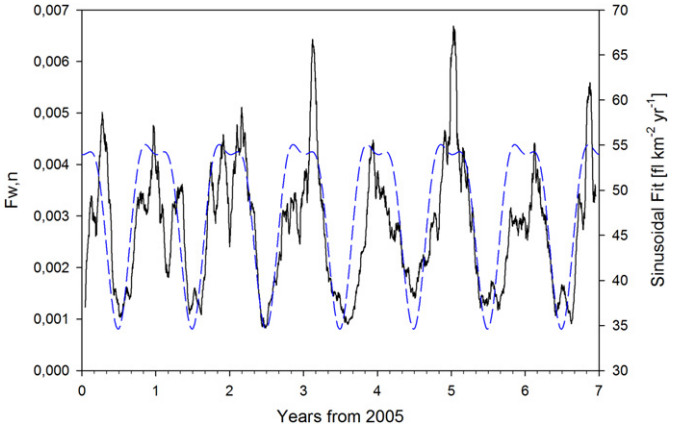

Fig. 6. Evolution of the $f_{w,n}$ for the Democratic Republic of the Congo (solid line) and the sinusoidal fit presented by Collier and Hughes (2011) (dashed line).

most of the African countries. The most intense lightning activity over Africa occurs in the Democratic Republic of the Congo, which lies entirely within the Congo River Basin. They proposed that the average annual variation in lightning can be represented by annual and semiannual sinusoidal components. Fig. 6 displays the daily evolution of the lightning activity of the Congo Basin. The daily value of the amount of lightning flashes (f_w) detected by WWLLN within the spatial window between $[-10^\circ;\ 5^\circ]$ of latitude and $[15^\circ;\ 30^\circ]$ of longitude was computed. Again, in order to take into account the variation in the detection efficiency of the WWLLN, the f_w values were normalized to the total number of flashes in the year. Thus the variable

$$f_{w,n} = \frac{f_w}{\sum_{\text{All year}} f_w}$$

is used as an indicator of the daily variation of the lightning activity of the region. Fig. 6 shows the moving average with 32 days of $f_{w,n}$ (black line) and the sinusoidal fit proposed by Collier and Hughes (2011a) for the Democratic Republic of the Congo (blue dashed line). The 32 days smoothing average of $f_{w,n}$ was chosen to remove the effect of day-to-day variations from the time series data and to create the equivalent of monthly averages (Aumann et al., 2006, 2007). Both curves show good temporal correlation with the minimum lightning activity around June. And, despite the semi- and annual component found by Collier and Hughes (2011a), both curves show a broad maximum extending from November to February. Although, the WWLLN is not capable of detecting the semiannual variation, it can detect the main features of the monthly variation in lightning activity and $f_{w,n}$ seems to be good indicator of this variation

The variable $f_{w,n}$ was also used to study the inter-annual characteristics of three different regions: the high-lightning activity center located between $[0^\circ;\ -3^\circ]$ of latitude and $[27^\circ;\ 29^\circ]$ of longitude (Fig. 7a), the central region limited by $[2^\circ;\ -5^\circ]$ of latitude and $[20^\circ;\ 25^\circ]$ of longitude (Fig. 7b), and the region over Lake Victoria (Fig. 7c). Fig. 7 shows the mean value of *fw,n* with a 32 days moving average of these three regions. The three regions present a similar annual variation with low amplitude and with less lightning activity between June and August. The high-lightning activity center (Fig. 7a) and the central region (Fig. 7b) show good correlation on the daily lightning variation with a Pearson coefficient of 0.83 ($p < 10^{-4}$). The annual variation at Lake Victoria is correlated to the high-lightning activity region and the central region with Pearson coefficients of 0.66 ($p < 10^{-4}$) and 0.57 ($p < 10^{-4}$), respectively. The main difference on the lightning activity variations of Lake Victoria and the Congo Basin is the peak around March and April observed over Lake Victoria. Throughout the year, the Congo Basin presents high temperatures, with mean values of ~300 K, and an annual range of ~6 °C and a diurnal range between 10° and 15 °C (Nicholson, 2001). In short time scales, several studies found a positive correlation between tropical lightning activity and surface air temperature (Price, 1993; Markson and Price, 1999; Price and Asfur, 2006). Therefore, the low amplitude between the high and lower lightning activity periods observed is consistent with the low range in the annual temperature of the region. Nicholson (2000) reported a rainy season over the Congo Basin lasting between 10 and 12 months with a maximum rainfall during November. The mean annual rainfall is higher than 1500 mm^{-1}, reaching 2000 mm^{-1} in the central region.

Lake Victoria presents substantial rainfall occurring throughout the year with a mean annual rainfall of 1200 mm^{-1} (Nicholson, 2000). Asnani (1993) found a quasi-permanent trough that lingers over Lake Victoria due to locally induced convection, orographic influence, and lake-land thermal contrast which tends to favor convection over the lake throughout the year. However, the seasonal rainfall over Lake Victoria shows a bimodal regime

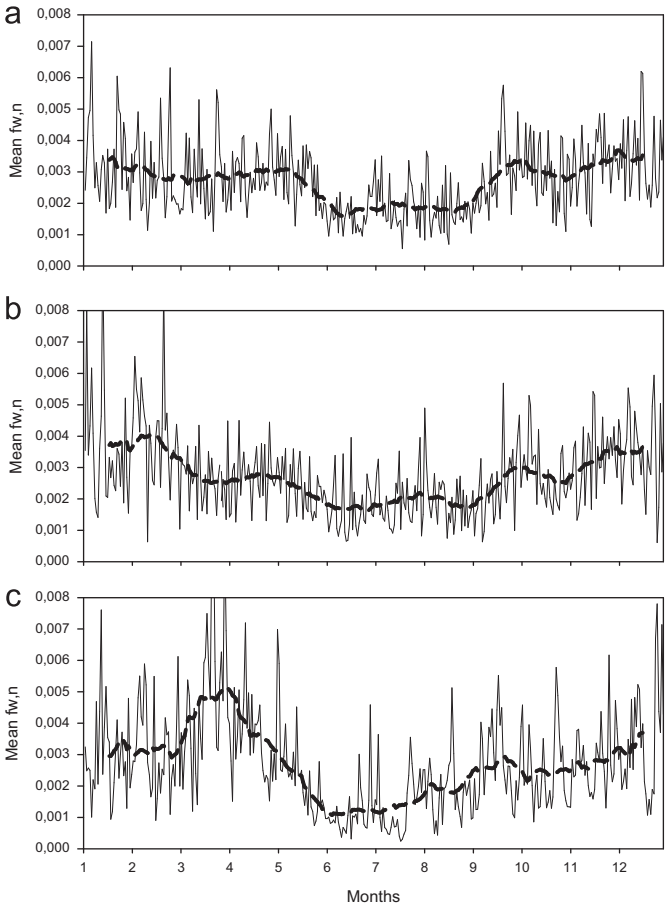

Fig. 7. Monthly evolution of the mean $f_{w,n}$ for (a) the high-lightning activity center on the eastern edge of the Congo Basin region enclosed within $[0^\circ;\ -3^\circ]$ of latitude and $[27^\circ;\ 29^\circ]$ of longitude, (b) the central region enclosed within $[2^\circ;\ -5^\circ]$ of latitude and $[20^\circ;\ 25^\circ]$ of longitude, and (c) for the region comprising the Lake Victoria.

which is mainly controlled by the north–south ITCZ migration across the region. This seasonal cycle shows a long rainy season between March and May, when the maximum value of rainfall is observed, and a short rainy season between October and December. Although the ITCZ migration seems to be controlling the seasonal rainfall over the regions, Collier and Hughes (2011b) found a weak relationship between equatorial lightning activity and the ITCZ over Africa. This seems to be due to the asymmetry in the moisture (water vapor) carried by the air moving into the ITCZ from the south (Congo Basin and Gulf of Guinea) and from the north (Sahara).

Fig. 8 shows the diurnal variation in lightning activity of the three regions analyzed in Fig. 7. The vertical bins represent the fraction of the total lightning during a whole year as a function of local time; counts are grouped into 1-h bins. The diurnal cycle of the high-lightning activity center and the central region (Fig. 8a and b) displays scarce lightning activity between 6:00 and 12:00 and a peaks between 16:00 and 20:00 local times. The diurnal cycle observed in the high lightning center and the central region is consistent with the global observation by LIS and the OTD, which show that tropical continental lightning has a clear diurnal peak in flash rate during the local afternoon (Williams et al., 2000).

On the other hand, the diurnal cycle of the lightning activity over Lake Victoria (Fig. 8c) shows little variation during the day. Two small peaks can be observed, one of them between 15:00 and 19:00 local time and another one between 23:00 and 05:00 local time, with lower lightning activity between 11:00 and 13:00 local

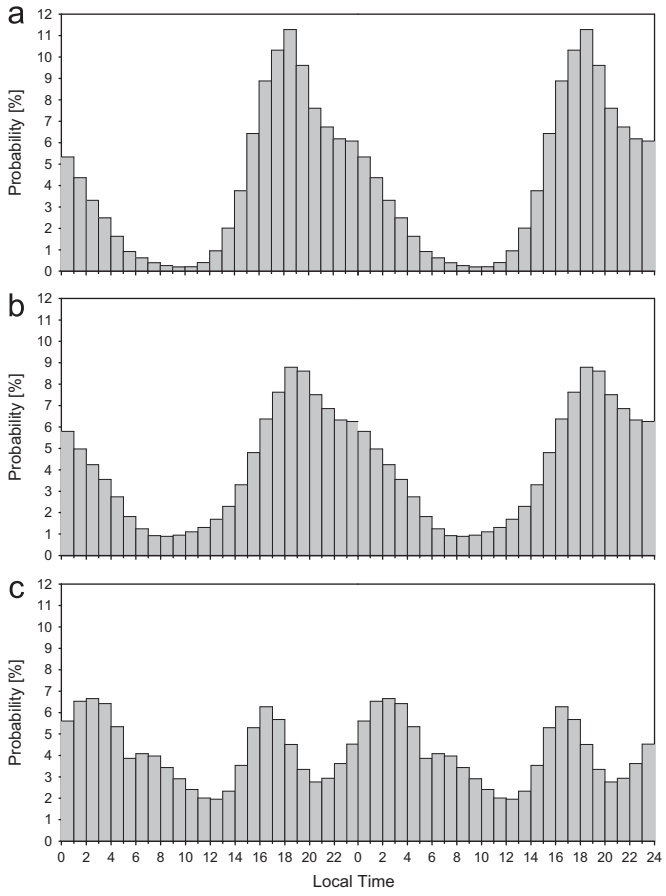

Fig. 8. Probability of the hourly distribution of *FRw* for (a) the high-lightning activity center on the eastern edge of the Congo Basin region enclosed within [0°; −3°] of latitude and [27°; 29°] of longitude, (b) the central region enclosed within [2°; −5°] of latitude and [20°; 25°] of longitude, and (c) for the region comprising the Lake Victoria.

time and between 20:00 and 22:00 local time. Ba and Nicholson (1998) studied the convective activity over the Rift Valley lakes on East Africa using satellite-derived convective indices and rainfall measurements. They found two maxima in the diurnal cycle of the convective activity over Lake Victoria, one during the morning and a second one in the afternoon. Fraedrich (1972), using a simple model, found a peak in the nocturnal circulation over Lake Victoria which generally occurs between midnight and early morning hours when the lake surface is warmer than the surrounding land area. Song et al. (2004), using a nested coupled model, found that the heat transport between the warmer and shallower southeastern sector of Lake Victoria to the colder pool of water over the northeastern sector, results in an asymmetric lake-surface temperature distribution. This temperature distribution modifies the overlying wind circulation over the Lake and induces a higher average surface temperature of the Lake. The increase in the evaporation area due to the higher surface temperature is compensated with the low-level atmospheric horizontal outflow, induced by the temperature gradient, resulting in a decrease in the cloud cover and rainfall over the Lake. The mean winds (Song et al., 2004) over Lake Victoria shows a diurnal cycle with lake breeze dominating during the afternoon and evening, and a strong land breeze at night and at early morning. This diurnal cycle, in conjunction with the Rift Valley topography, produces a more intense rainfall region over the east of Lake Victoria, which could explain the lower lightning activity over the warmer sector of the Lake.

4. Conclusion

The LIS results report that the Congo basin in Africa has the highest lightning activity, throughout the year, with resultant flash densities exceeding 50 fl km^{-2} yr^{-1}. The lightning activity over this region presents a pattern with a localized center of high lightning activity located on the western foot of the Albertine Rift. This center is located between [0°; −3°] of latitude and [27°; 29°] of longitude and has a flash rate density exceeding 100 fl km^{-2} yr^{-1}. Results seem to indicate that the topographic relief forces air upwards that further enhances thunderstorm development and can subsequently lead to an increase in lightning activity.

The Congo Basin shows high surface air temperature, low values of the cloud top temperature and substantial annual rainfall. The low amplitude in the lightning annual variations is consistent with the low annual variation of temperatures in the region and with a rainy season lasting almost all year long. The diurnal cycle observed is consistent with global observation for tropical region with a peak in flash rate in the late afternoon (local time) and with the rainfall diurnal cycle.

Significant lightning activity was also found over Lake Victoria which presents similar daily variation in flash rate and a diurnal lightning activity without a marked cycle.

Lightning activity is related to atmospheric convection which occurs due to the heating of the boundary layer by solar radiation during the day or by the mixing of air masses of different densities. Also, topographic forcing can initiate instabilities that trigger the thunderstorm formation.

Acknowledgments

The authors wish to thank the World Wide Lightning Location Network (http://wwlln.net), collaboration among over 50 universities and institutions, for providing the lightning location data used in this paper.

This work was supported by SECYT-UNC, CONICET and FONCYT.

References

Abreu, D., Chandan, D., Holzworth, R.H., Strong, K., 2010. A performance assessment of the WorldWide Lightning Location Network (WWLLN) via comparison with the Canadian Lightning Detection Network (CLDN). Atmospheric Measurement Techniques 3, 1143–1153.

Albrecht, R.I., Goodman, S.J., Petersen, W.A., Buechler, D.E., Bruning, E.C., Blakeslee, R.J. and Christian, H.J., 2011. The 13 years of TRMM lightning imaging sensor: from individual flash characteristics to decadal tendencies, XIV International Conference on Atmospheric Electricity, August 08-12, 2011, Rio de Janeiro, Brazil.

Asnani, G.C., 1993. Tropical meteorology. Indian Institute of Tropical Meteorology, Pune.

Aumann, H.H., Broberg, S.D., Elliott, Gaiser, S., Gregorich, D., 2006. Three years of atmospheric infrared sounder radiometric calibration validation using sea surface temperatures. Journal of Geophysical Research: Atmospheres 111, D16S90, http://dx.doi.org/10.1029/2005JD006822.

Aumann, H.H., Gregorich, D.T., Broberg, S.E., Elliott, D.A., 2007. Seasonal correlations of SST, water vapor, and convective activity in tropical oceans: a new hyperspectral data set for climate model testing. Geophysical Research Letters 34, L15813, http://dx.doi.org/10.1029/2006GL029191.

Ávila, E.E., Bürgesser, R.E., Castellano, N.E., Collier, A.B., Compagnucci, R.H., Hughes, A.R.W., 2010. Correlations between deep convection and lightning activity on a global scale. Journal of Atmospheric and Solar-Terrestrial Physics 72 (14–15), 1114–1121.

Ba, M.B., Nicholson, S.E., 1998. Analysis of convective activity and its relationship to the rainfall over the rift valley lakes of East Africa during 1983–1990 using the meteosat infrared channel. Journal of Applied Meteorology 37, 1250–1264.

Boccippio, D.J., Goodman, S.J., Heckman, S., 2000. Regional differences in tropical lightning distributions. Journal of Applied Meteorology 39, 2231–2248.

Boccippio, D.J., Koshak, W.J., Blakeslee, R.J., 2002. Performance assessment of the optical transient detector and lightning imaging sensor. Part I: predicted diurnal variability. Journal of Atmospheric and Oceanic Technology 19, 1318–1332.

Brooks, C.E.P., 1925. The distribution of thunderstorms over the globe. Geophysical Memoirs London 24, 147–164.
Bürgesser, R.E., Nicora, M.G., Ávila, E.E., 2012. Characterization of the lightning activity of "Relámpago del Catatumbo". Journal of Atmospheric and Solar-Terrestrial Physics 77, 241–247.
Chahine, M.T., et al., 2006. The atmospheric infrared sounder (AIRS): improving weather forecasting and providing new data on greenhouse gases. Bulletin of the American Meteorological Society 87, 911–926.
Christian, H.J., Blakeslee, R.J., Goodman, S.J., Mach, D.A., Stewart, M.F., Buechler, D.E., Koshak, W.J., Hall, J.M., Boeck, W.L., Driscoll, K.T. and Boccippio, D.J., 1999. The lightning imaging sensor. Proceedings of the Eleventh International Conference on Atmospheric Electricity, Huntsville, AL, NASA, 746–749.
Christian, H.J., Blakeslee, R.J., Boccippio, D.J., Boeck, W.L., Buechler, D.E., Driscoll, K.T., Goodman, S.J., Hall, J.M., Koshak, W.J., Mach, D.M., Stewart, M.F., 2003. Global frequency and distribution of lightning as observed from space by the optical transient detector. Journal of Geophysical Research 108, 4005, http://dx.doi.org/10.1029/2002JD002347.
Collier, A.B., Hughes, A.R.W., 2011a. A harmonic model for the temporal variation of lightning activity over Africa. Journal of Geophysical Research, 116.
Collier, A.B., Hughes, A.R.W., 2011b. Lightning and the African ITCZ. Journal of Atmospheric and Solar-Terrestrial Physics 73 (16), 2392–2398.
Dowden, R.L., Brundell, J.B., Rodger, C.J., 2002. VLF lightning location by time of group arrival (TOGA) at multiple sites Source. Journal of Atmospheric and Solar-Terrestrial Physics 64 (7), 817–830.
Dowden, R.L., Holzworth, R.H., Rodger, C.J., Lichtenberger, J., Thomson, N.R., Jacobson, A.R., Lay, E.H., Brundell, J.B., Lyons, T.J., O'Keefe, S., Kawasaki, Z., Price, C., Prior, V., Ortega, P., Weinman, J., Mikhailov, Y., Woodman, R., Qie, X., Burns, G., Collier, A.B., Pinto Jr, O., Diaz, R., Adamo, C., Williams, E.R., Kumar, S., Raga, G.B., Rosado, J.M., Ávila, E.E., Clilverd, M.A., Ulich, T., Gorham, P., Shanahan, T.J.G., Osipowicz, T., Cook, G., Zhao, Y., Oct. 2008. World-Wide lightning location using VLF propagation in the Earth-Ionosphere waveguide. IEEE Antennas and Propagation Magazine 50 (5), 40–60.
Fraedrich, K., 1972. A simple climatological model of the dynamics and energetics of the nocturnal circulation at Lake Victoria. Quarterly Journal of the Royal Meteorological Society 98, 322–335, http://dx.doi.org/10.1002/qj.49709841606.
Fu, R., Genio, A.D.D., Rossow, W.B., 1990. Behavior of deep convective clouds in the tropical Pacific deduced from ISCCP radiances. Journal of Climate 3, 1129–1152.
Hong, G., Heygster, G., Miao, J., Kunzi, K., 2005. Detection of tropical deep convective clouds from AMSU-B water vapor channels measurements. Journal of Geophysical Research, 110, http://dx.doi.org/10.1029/2004JD004949.
Jacobson, A.R., Holzworth, R.H., Harlin, J., Dowden, R.L., Lay, E.H., 2006. Performance assessment of the World Wide Lightning Location Network (WWLLN), using the Los Alamos Sferic Array (LASA) array as ground-truth. Journal of Atmospheric and Oceanic Technology 23, 1082–1092.
Lay, E.H., Holzworth, R.H., Rodger, C.J., Thomas, J.N., Pinto Jr., O., Dowden, R.L., 2004. WWLL global lightning detection system: regional validation study in Brazil. Geophysical Research Letters 31, L03102, http://dx.doi.org/10.1029/2003GL018882.
Liu, G., Curry, J.A., Sheu, R.-S., 1995. Classification of clouds over the western equatorial Pacific Ocean using combined infrared and microwave satellite data. Journal of Geophysical Research 100, 13,811–13,826.
Markson, R., Price, C., 1999. Ionospheric potential as a proxy index for global temperatures. Atmospheric Research 51, 309–314.
Nicholson, S.E., 2000. The nature of rainfall variability over Africa on time scales of decades to millenia. Global and Planetary Change 26 (1–3), 137–158.
Nicholson, S.E., 2001. Climatic and environmental change in Africa during the last two centuries. Climate Research, 17.
Price, C., Rind, D., 1992. A simple lightning parameterization for calculating global lightning distributions. Journal of Geophysical Research, 9919–9933.
Price, C., 1993. Global surface temperatures and the atmospheric electrical circuit. Geophysical Research Letters 20, 1363–1366.
Price, C., Asfur, M., 2006. Can lightning observations be used as an indicator of uppertropospheric water vapor variability? Bulletin of the American Meteorological Society 87, 291–298.
Rodger, C.J., Brundell, J.B., Dowden, R.L., 2005. Location accuracy of VLF World Wide Lightning Location (WWLL) network: post-algorithm upgrade. Annales Geophysicae 23, 277–290.
Rodger, C.J., Brundell, J.B., Holzworth, R.H., and Lay, E.H., 2009. Growing detection efficiency of the World Wide Lightning Location Network. American Institute of Physics Conference Proceedings, Coupling of thunderstorms and lightning discharges to near-Earth space: Proceedings of the Workshop, 23–27 June 2008, Corte, France, 1118, 15–20, http://dx.doi.org/10.1063/1.3137706.
Song, Y., Semazzi, F.H.M., Xie, L., Ogallo, L.J., 2004. A coupled regional climate model for the Lake Victoria basin of East Africa. International Journal of Climatology 24, 57–75, http://dx.doi.org/10.1002/joc.983.
Ushio, T., Heckman, S.J., Boccippio, D.J., Christian, H.J., Kawasaki, Z.I., 2001. A survey of thunderstorm flash rates compared to cloud top height using TRMM satellite data. Journal of Geophysical Research 106 (D20), 24089–24095.
Whipple, F.J.W., 1929. On the association of the diurnal variation of electric potential gradient in fine weather with the distribution of thunderstorms over the globe. Quarterly Journal of Royal Meteorological Society 55, 1–17.
Williams, E.R., 1985. Large-scale charge separation in thunderclouds. Journal of Geophysical Research 90, 6013–6025.
Williams, E.R., Rothkin, K., Stevenson, D., Boccippio, D., 2000. Global lightning variations caused by changes in thunderstorm flash rate and by changes in the number of thunderstorms. Journal of Applied Meteorology 39, 2223–2230, http://dx.doi.org/10.1175/1520-0450.
Williams, E.R., Satori, G., 2004. Lightning, thermodynamic and hydrological comparison of the two tropical continental chimneys. Journal of Atmospheric and Solar-Terrestrial Physics 66, 1213–1231.